



Quantitative probing of hydrogen environments in quasicrystals by high-resolution NMR spectroscopy



Jin Jung Kweon^a, Hyo-Im Kim^{a,b}, Sang-hwa Lee^{c,1}, Jaeyong Kim^{c,*}, Sung Keun Lee^{a,d,*}

^a Laboratory of Physics and Chemistry of Earth Materials, School of Earth and Environmental Sciences, Seoul National University, Seoul 08826 South Korea

^b Department of Geology and Research Institute of Natural Science, Gyeongsang National University, Jinju 52828 South Korea

^c Department of Physics, Institute for High Pressure, Hanyang University, Seoul 04763 South Korea

^d College of Natural Sciences, Institute of Applied Physics, Seoul National University, Seoul 08826 South Korea

ARTICLE INFO

Article history:

Received 21 October 2021

Revised 10 December 2021

Accepted 12 January 2022

Available online 20 January 2022

Keywords:

Hydrogenated quasicrystals

Hydrogen storage

High-resolution ^1H NMR under fast

spinning

ABSTRACT

Metal-based quasicrystals with unique quasi-periodic atomic arrangements are known to store a large amount of hydrogen under reasonable pressure and temperature for practical application as energy storage materials. While details on the atomic environments around hydrogen are central to understanding their hydrogen-storage capacity, the experimental probing of hydrogen environments and direct estimation of hydrogen content in hydrogen-bearing metal compounds, including quasicrystals, remain the holy grail in metallurgy and materials science because of the lack of suitable spectroscopic probes of hydrogen in noncrystalline metal alloys. While ^1H nuclear magnetic resonance (NMR) measurement under *fast spinning* has the potential to reveal the nature of bonding around hydrogen, applying NMR to these metallic compounds has been challenging. Here, we report the first ^1H nuclear magnetic resonance (NMR) spectra of hydrogenated quasicrystals under fast sample spinning, revealing previously unknown details of the bonding environment and hydrogen content. The NMR spectra of TiZrNi quasicrystals show that the metal atoms in the first coordination shell of neutral hydrogen shift gradually from Zr to Ti to Ni with increasing hydrogen content. This trend accounts for Ni-induced increase in the hydrogen-storage capacity and the enhanced desorption kinetics observed near ambient conditions. The ^1H peak maximum shifted linearly toward lower frequencies with increasing hydrogen content, highlighting the utility of fast-spinning NMR as a novel quantitative probe of hydrogenated quasicrystals. These results open a new window to access the nature of hydrogen and its content in diverse hydrogen-bearing energy materials based on metal alloys using high-resolution ^1H NMR spectroscopy, providing improved prospects for the hydrogen economy.

© 2022 The Authors. Published by Elsevier Ltd on behalf of Acta Materialia Inc.

This is an open access article under the CC BY-NC-ND license

(<http://creativecommons.org/licenses/by-nc-nd/4.0/>)

1. Introduction

Quasicrystals are characterized by unique quasiperiodic atomic arrangements, such as fivefold rotational symmetry, that cannot be explained by the classical concept of crystalline materials [1]. While natural quasicrystals have been found in meteorites [2,3], quasicrystals have primarily been synthesized by melting and rapid quenching from liquids (on the order of 10^4 – 10^7 K/s) [4,5] and/or through shock compression [6]. Quasicrystals are known to have

potential applications as hydrogen storage materials [7], which could be used in clean and renewable energy systems [8–11]. Indeed, high-performance hydrogen storage materials consist of composite metal alloys and their hydrides (e.g., Refs. [12–15]; see Supplementary Information, SI-1 for metal-bearing hydrogen storage materials). In particular, TiZr-based quasicrystals are among the most effective hydrogen-absorbing materials because the binding energy between hydrogen and metal atoms is expected to be not significant, facilitating efficient removal of absorbed hydrogen [16–23]. Furthermore, the number of interstitials (i.e., potential sites for hydrogen) in quasicrystals is greater than those in crystalline metal alloys and other candidate materials [18,24]. In fact $\text{Ti}_{53}\text{Zr}_{27}\text{Ni}_{20}$ quasicrystals store hydrogen up to hydrogen to host metal atom ratio (H/M) of 1.79 (i.e., 179 absorbed hydrogen atoms per 100 metal atoms) [17,18].

* Corresponding author.

** Corresponding author at: School of Earth and Environmental Sciences, Seoul National University, Seoul 08826, South Korea (<https://g2mat.snu.ac.kr>).

E-mail addresses: kimjy@hanyang.ac.kr (J. Kim), sungklee@snu.ac.kr (S.K. Lee).

¹ Present address: Research Center for Materials, Advanced Institute of Convergence Technology, Suwon 16229 South Korea.

Despite its importance, the nature of the interaction between hydrogen and the quasicrystalline lattice remains to be explored, whereas earlier theoretical studies suggested that hydrogen atoms occupy one of the low-energy tetrahedral sites, consisting primarily of Ti and Zr [25,26]. Detailed experimental probing of the hydrogen environments and their bonding nature in quasicrystals has been challenging because of the lack of a suitable experimental probe for absorbed hydrogen. Furthermore, *direct* and precise estimation of the hydrogen content in hydrogen-bearing metal compounds, including metal hydrides and quasicrystals, is not trivial; while volumetric and gravimetric methods have commonly been used to determine the hydrogen content [27], the methods may not be suitable for detecting a small amount of hydrogen (e.g., ~mg). Since the quasicrystalline lattice tends to expand with increasing hydrogen concentration [18,21], X-ray diffraction (XRD) data from quasicrystals are useful for inferring the hydrogen content. However, the lack of a crystalline lattice in quasicrystals may not allow a *direct* inference of the hydrogen content.

Solid-state nuclear magnetic resonance (NMR) spectroscopy provides element-specific information on the local structures and environments around target nuclides in diverse diamagnetic materials [28,29]. This technique has also been useful for studying paramagnetic-element-bearing (e.g., Fe and Mn) crystalline oxides [30–32] and disordered materials [33–36]. In particular, ^1H NMR can potentially probe the nature of the bonding in diverse metal hydrides [36]. An earlier ^1H static (without sample spinning) NMR study confirmed that hydrogen in TiH_x and ZrH_x tends to have negative ^1H NMR Knight shifts [37] that result from the modification of the local static field around ^1H due to the interaction with conduction electrons through hyperfine coupling [36,38]. Pioneering ^1H NMR studies on quasicrystals and metallic glasses were mainly conducted under *static* conditions [22,39,40], and the application of ^1H NMR to these metallic compounds for hydrogen storage materials, including quasicrystals, focused primarily on the study of spin relaxation times and related transport properties [41–43]. Consequently, the peaks in these *static* ^1H NMR studies were often quite broad because anisotropic ^1H – ^1H dipolar spin coupling is dominant, and thus, the detailed atomic configurations around hydrogen are hidden. Fast magic-angle spinning (MAS) effectively removes ^1H – ^1H dipolar interactions (e.g., [44]). Advances in solid-state NMR under fast spinning speeds have enabled the collection of high-resolution ^1H NMR spectra, providing site-specific information about hydrogens in various materials [45–52]. However, ^1H MAS NMR spectra from quasicrystals under fast sample spinning are not currently available, as the magnetic permeability of quasicrystals is larger than 1 (~1.2 at 100 K for $\text{Ti}_{50}\text{Zr}_{33}\text{Ni}_{17}$ quasicrystals) [53], making spinning of the sample under a magnetic field difficult. Therefore, high-resolution NMR scans from hydrogen-bearing quasicrystals have been anticipated. In this study, we report the first high-resolution ^1H MAS NMR spectra of $\text{Ti}_{53}\text{Zr}_{27}\text{Ni}_{20}$ quasicrystals with different H/M ratios (from 0.5 to 1.8) under fast spinning speeds up to 35 kHz, yielding new insights into detailed hydrogen environments with varying hydrogen contents. Based on the high-resolution NMR results, we also aim to develop a structural proxy for the hydrogen content in quasicrystals.

2. Experimental

Sample preparation. $\text{Ti}_{53}\text{Zr}_{27}\text{Ni}_{20}$ quasicrystals were synthesized through arc melting of mixed elements consisting of Ti, Zr, and Ni metals at a temperature of ~2000 °C in an argon environment on a Cu hearth (see Ref. [18] for further details). The resulting ingot was remelted several times to ensure homogeneous mixing of the elements. The melts were quenched on stainless steel wheel with a rotation frequency of 50 Hz. Thin metallic ribbons of quasicrystals

were produced via fast quenching at a cooling rate of ~10⁶ °C/s. The quasicrystal samples confirmed by XRD were etched by Ar plasma, which removes the surface oxygen layers. After additional surface treatment with a Pd coating, hydrogen insertion was performed. Samples having desired amounts of hydrogen (H/M = 0.5, 0.7, 0.75, 0.9, and 1.8) were prepared by employing an automatic gas-handling system at 300 °C [18]. The hydrogen content in the sample was determined by two independent methods: (1) measuring the mass gain after hydrogenation and (2) calculating the number of moles of hydrogen after hydrogen uptake in a known volume of the sample chamber.

NMR spectroscopy. ^1H NMR experiments of $\text{Ti}_{53}\text{Zr}_{27}\text{Ni}_{20}$ quasicrystals were performed on a Bruker NMR system (14.1 T) at a Larmor frequency of 600.41 MHz at Seoul National University. The spectra were collected with a 1.9 mm triple-resonance Bruker NMR probe with varying spinning speeds from 10 to 35 kHz. To remove potential ^1H probe background signals, the spin-echo pulse sequence ($\pi/2\text{-}t\text{-}\pi\text{-}t$) was used [54,55]. The $\pi/2$ pulse lengths were 3 μs for H/M = 1.8 and 1.5 μs for the other samples. Considering the estimated spin-lattice relaxation times (T_1) of 0.4–0.5 s, a relaxation delay of 3 s was used. The *Korringa relaxation* may play a role in the current spin-relaxation processing involving metal element. Nevertheless, as the effect becomes prevalent in spin-lattice relaxation at lower temperature condition, the current spin-lattice relaxation process at high temperature may not be mainly affected by the electron-correlation effects (See SI-2 for T_1 measurement). All ^1H NMR spectra were referenced to an external tetramethylsilane (TMS) solution. The powdered quasicrystals needed higher air pressure for spinning the samples due to the dynamo current induced by the samples: fast spinning of large amounts of powdered quasicrystal samples (e.g., >~10 mg) is challenging. Therefore, for high spinning speeds greater than 30 kHz, ~2–5 mg of sample was used. To maximize the signal intensity, the sample was located at the center of the rotor with dried Teflon tape as an insert in the 1.9 mm NMR rotor. The Teflon tape was heated at 200 °C for 30 min to remove any hydrous impurity phase often observed at ~0–5 ppm in the ^1H NMR spectrum. Variable-temperature ^1H NMR measurements were performed using a 1.9 mm Bruker NMR probe coupled with external air heating at a spinning speed of 10 kHz [56]. Therefore, the heating is not localized only to the sample but to rotor. The sample temperature was also estimated using the ^{207}Pb MAS NMR shift of a $\text{Pb}(\text{NO}_3)_2$ sample [56]. Because high temperature experiments are difficult to perform under fast MAS, a spinning speed of 10 kHz was used. We note that under fast MAS, the friction-induced heating increases the sample temperature, which was then used to explore the effect of temperature at a spinning speed of 35 kHz (SI-3). The sample volume is very small (~5 mg). We were able to locate the sample in the middle of the rotor. Therefore, the temperature gradient within the sample is likely to be minor.

3. Results and discussions

3.1. Hydrogen environments in $\text{Ti}_{53}\text{Zr}_{27}\text{Ni}_{20}$ quasicrystals: insights from ^1H NMR

^1H MAS NMR results. The ^1H static NMR spectra of $\text{Ti}_{53}\text{Zr}_{27}\text{Ni}_{20}$ quasicrystals (Fig. 1A) show a slight negative peak shift with increasing hydrogen content. This suggests changes in the hydrogen environment and the magnitude of the interaction between hydrogen and the nearby host metal elements. The shift in peak position is also attributed to the change in the polarization of the hydrogen 1 s orbital arising from the d-electrons of the metal elements in the quasicrystal [57,58]. The peak width increases with increasing hydrogen content and is 28, 30, and 34 kHz for H/M ratios of 0.5, 0.9, and 1.8, respectively. Such an increase in the peak width in the

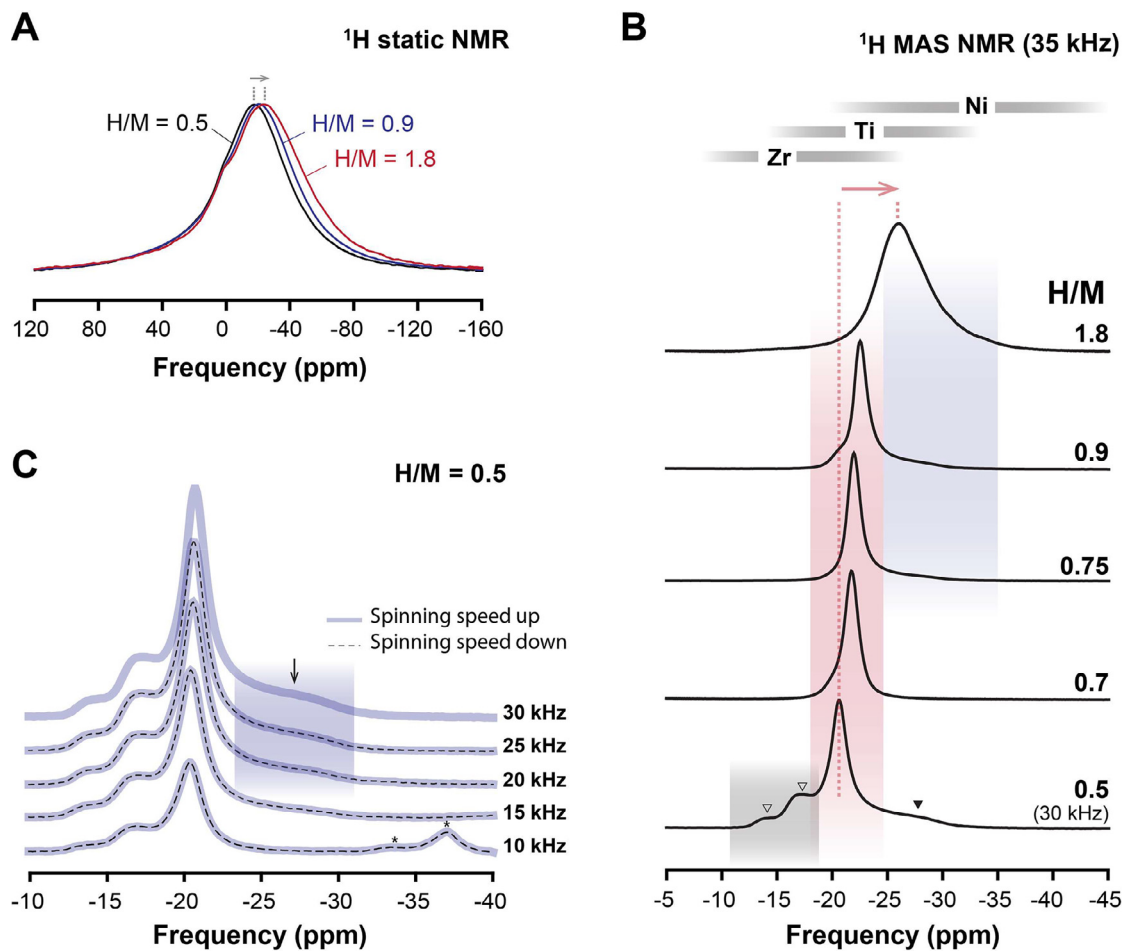


Fig. 1. (A) ¹H static spectra (at 14.1 T) of Ti₅₃Zr₂₇Ni₂₀ quasicrystals with different H/M ratios (0.5, 0.9, and 1.8). (B) ¹H MAS NMR spectra (at 14.1 T) obtained using a spinning speed of 30 kHz for H/M = 0.5 and 35 kHz for Ti₅₃Zr₂₇Ni₂₀ quasicrystals with H/M ratios of 0.7, 0.75, 0.9, and 1.8. (C) ¹H MAS NMR spectra of the Ti₅₃Zr₂₇Ni₂₀ quasicrystals with H/M = 0.5 at different spinning speeds for both spinning up (thick solid lines) and spinning down (thin dotted lines). The asterisks (*) indicate the spinning sidebands due to dipolar interaction are shown. See SI-4 for the spectrum with larger spectral width where multiple spinning sideband patterns are shown.

static NMR spectra partly indicates that the dipole–dipole interaction between ¹H spins increases with increasing H/M ratio. Nevertheless, owing to the broad peak width in the spectra, detailed structural insights could not be obtained.

The fast sample spinning speed of 30–35 kHz (which is larger than the peak width in the static spectra) effectively reduces the peak broadening due to anisotropic spin interactions. Fig. 1B shows the ¹H MAS NMR spectra of Ti₅₃Zr₂₇Ni₂₀ quasicrystals with varying hydrogen concentrations (H/M from 0.5 to 1.8) under fast rotor spinning speed, revealing the evolution of multiple hydrogen sites in the Ti₅₃Zr₂₇Ni₂₀ quasicrystals. Fig. 1C also shows the ¹H MAS NMR spectra for H/M = 0.5 at various spinning speeds (as the spinning speed is increased from 10 kHz to approximately 35 kHz). The increase in the sample spinning speed reduces the magnitude of the ¹H–¹H dipolar interaction, leading to an increase in the ratio of the central band to the total intensity (see SI-5 and Fig. S5 for H/M from 0.9 to 1.8). Above 30 kHz, the peak shape (including intensity) is invariant, suggesting that a speed of approximately 30 kHz is sufficient to reduce the ¹H–¹H dipolar interaction in the hydrogenated quasicrystals, unveiling *multiple* hydrogen sites. Intriguingly, the ¹H peak maximum shifts toward lower frequencies with increasing hydrogen content, from -21 ppm (H/M = 0.5) to -26 ppm (H/M = 1.8). The negative shift may result from an increase in electron density of the *d*-orbital [57]. The changes in the peak position with increasing H/M also demonstrate the evolution of the hydrogen environments and the changes in

the magnitude of the interactions between electrons and nuclear spins.

Peak assignment. As this manuscript reports the first application of high-resolution fast-spinning ¹H NMR to any quasicrystal consisting of metal elements and/or metal hydrides, we discuss in detail the origin of the peaks observed in the ¹H MAS NMR spectra for the quasicrystals. First, earlier theoretical and diffraction studies suggested that tetrahedral interstitial sites are predominant in Ti₅₃Zr₂₇Ni₂₀ quasicrystals [39,59]. The previous theoretical study of Ti₄₅Zr₃₈Ni₁₇ quasicrystals based on the canonical cell-tiling model showed that a large number of such tetrahedral sites were formed by Ti and Zr atoms [39,60]. In the current study, taking only a uniform distribution of Ti, Zr, and Ni around tetrahedral sites in Ti₅₃Zr₂₇Ni₂₀ into account, there are multiple dominant tetrahedral configurations around hydrogen, such as Ti₂ZrNi (18.2%), Ti₃Zr (16.1%), Ti₂Zr₂ (12.3%), Ti₃Ni (11.9%), TiZr₂Ni (9.3%), and Ti₄ (7.9%) (Fig. S6, SI-6). The detailed elemental mixing behavior could somewhat deviate from a random distribution; while Ti and Zr may show ideal mixing behavior, Ti–Ni and Zr–Ni in the quasicrystals exhibit enhanced proximity [60]. This leads to a decrease in the configurations mainly consisting of Ni. Furthermore, previous structural refinement of the icosahedral TiZrNi quasicrystal with a H/M of 0.3 suggested that the hydrogen atoms may have proximity to both Ti and Zr atoms in tetrahedral clusters [25]. Therefore, the observed changes in the ¹H peak shift in the quasicrystal are attributed to the structural diversity in tetrahedral in-

terstitial sites consisting of Zr, Ti, and Ni atoms near hydrogen with varying hydrogen content.

Second, the peak at approximately -28 ppm (solid reverse triangle in Fig. 1B) evolves with the increase in hydrogen concentration H/M from 0.5 to 1.8 . Particularly, the ^1H peak width abruptly increases with increasing H/M from 0.9 to 1.8 , partly because of the increase in the intensity of the broad component with a Lorentzian peak shape at ~ -28 ppm in the ^1H MAS NMR spectrum at $H/M = 1.8$. Previous NMR studies showed that the Lorentzian peak broadening is primarily due to the strong interaction between the unpaired electrons in the d -orbitals of paramagnetic elements (i.e., Ni) and the nuclear spins (i.e., paramagnetic effect) [32,61]. Furthermore, the integrated spectral intensity normalized to the sample mass for $H/M = 1.8$ is similar to that for $H/M = 0.9$ (despite the much larger hydrogen content for the former). Such a reduction in NMR peak intensity for the former is also characteristic of the paramagnetic effect, suggesting proximity between hydrogen and Ni. While further theoretical confirmation is needed to corroborate the current peak assignments, the broad peak at ~ -28 ppm indicates that hydrogen atoms have been in proximity to Ni (corresponding to hydrogen in tetrahedral sites consisting of Ni together with Ti and Zr).

Third, the variations in the Knight shifts with varying H/M are also due to the changes in the types of metal elements around the hydrogen. Earlier ^1H static NMR studies of ZrH_x [37,57] showed that the ^1H NMR shifts of hydrogen atoms in the tetrahedral sites consisting of Zr in ZrH_x varied from ~ -20 ppm (for $x = 0.9$) to ~ -80 ppm (for $x = 1.8$), while those in TiH_x exhibited more negative ^1H NMR Knight shifts in the range of approximately -60 ppm (for $x = 1.1$) to approximately -160 ppm (for $x = 2.0$) [37,58]. The larger negative ^1H NMR Knight shifts originated from the higher density of d -electron states in TiH_x and higher hydrogen concentration [37]. Thus, considering only the peak position in the current spectra, the hydrogen atoms in the quasicrystals may be positioned in the interstitial sites consisting mainly of Zr atoms [23,62]. However, we note that such a pronounced negative shift is not observed in the current study (Fig. 1A), indicating that the nature of hydrogen in the quasicrystals differs from that in the metal hydrides.

The NMR peak position in the ^1H NMR spectra for metal hydrides depends on the magnitude of the interactions between the hydrogen and d -electrons in the nearby metal cations; for example, stronger hydrogen-Ti interactions in the crystal lead to a more pronounced negative shift in the ^1H NMR spectra [37], while weaker hydrogen-Ti interactions in quasicrystals could lead to a smaller shift. The observed range of NMR peak positions and the magnitude of the change in the peak position (~ 5 ppm) for the TiZrNi quasicrystal with varying hydrogen content is much smaller than those for ZrH_x and TiH_x [37]. These results suggest that the dipolar interaction between hydrogen and these metal elements is sufficiently weaker than those reported for TiH_x [37]. The Ti-H distance in the quasicrystal is indeed considerably longer than that reported for TiH_x [63,64]; the Ti-H distance in TiH_x is ~ 1.92 Å, and that in $\text{Ti}_{53}\text{Zr}_{27}\text{Ni}_{20}$ alloys can be up to ~ 2.57 Å [63,64]. An increase in the metal-H bond length indicates a decrease in the magnitude of the dipolar interaction. Such trends comply well with the implications from the NMR peak shift, confirming that the hydrogen atoms in the quasicrystal are likely to be weakly bonded to these metal elements.

We also note that the spectrum for the quasicrystal with $H/M = 0.5$ exhibits multiple ^1H NMR peaks at -14 , -17 , and -27 ppm, together with the main ^1H peak at ~ -21 ppm. This indicates that the hydrogen atoms are in structurally inequivalent configurations in interstitial tetrahedral sites with varying number of Ti and Zr atoms (SI-6), suggesting a moderate extent of chemical disorder in the hydrogen distribution in the $H/M = 0.5$ sam-

ple. While they are not as clear as that for $H/M = 0.5$, the spectra for $H/M = 0.7$ and 0.9 resolve at least two distinct hydrogen sites (one at -21 ppm and the main peak at -23 ppm; the peak position moves with hydrogen content), corresponding to the heterogeneous hydrogen configurations. Because sites with more Zr atoms show smaller negative shifts than those with more Ti atoms, the peaks at -14 and -17 ppm correspond to hydrogen atoms in the tetrahedral sites specifically consisting of a larger number of Zr atoms. The noticeable change in the spectra with increasing hydrogen content from $H/M = 0.5$ to 0.7 suggests that there could be a threshold hydrogen concentration at which the hydrogen distribution in the quasicrystal changes abruptly with a slight change in hydrogen content. An increase in the hydrogen concentration above this threshold could lead to a decrease in the dispersion in the hydrogen sites, as the enhanced repulsive hydrogen-hydrogen interaction due to the increase in the hydrogen concentration would result in rearrangement of hydrogen atoms.

Taking all the factors and available information (statistical distribution of available tetrahedral sites, peak positions, and magnitude of metal-hydrogen interactions) into consideration, the changes in the peak position and shape in the NMR spectra with varying H/M enable identification of the nature of the hydrogen environments; specifically, the broad peak at -26 ppm corresponds to the hydrogen interacting more with Ni and/or Ti, while the peak at ~ -21 ppm corresponds to the hydrogen site that is weakly bound mainly to Zr and/or Ti. Therefore, the metal element around the hydrogen in the quasicrystals changes preferentially from Zr to Ti to Ni as the hydrogen concentration increases. The current ^1H MAS NMR experiment under fast spinning speed (> 30 kHz) highlights the utility of fast-spinning MAS as a new probe for determining the local structure of quasicrystals.

Note that the NMR shift ranges and corresponding peak widths in the ^1H NMR spectra allow us to identify whether hydrogen tends to form molecular hydrogens (H_2). The ^1H NMR peak positions of molecular hydrogen trapped inside open-cage fullerenes and C_{70} fullerene cages are -7.5 ppm and -24.7 ppm, respectively [65,66]. However, the full widths at half maximum (FWHM) of the peaks in the ^1H static NMR spectra for mobile hydrogen molecules are several kHz, whereas the peaks in the ^1H static NMR spectra of quasicrystals in the current study and of metal hydrides in general are broad, with an FWHM of approximately 30–40 kHz, because of the moderate degree of dipolar interactions between ^1H [39,67]. Their broad linewidths indicate that the hydrogen in the quasicrystals exists as atomic-state hydrogen, not molecular hydrogen (SI-7). As also indicated from the spectra for the annealed quasicrystals, we note that the observed peak is not due to surface-adsorbed water or hydroxyl species (SI-8) [68]. Further justification of the current peak assignment is provided in the Supplementary Information (see SI-7). We note that the hydrogen environments of the H-bearing quasicrystals with varying composition (Zr, Ni, Ti content) and diverse hydrogen content, particularly with lower hydrogen content ($H/M < 0.5$) and those between $H/M = 0.9$ and $H/M = 1.8$ remains to be explored. While the current interpretation of the hydrogen environments is not fully qualitative, more extensive ^1H NMR data allows us to have more quantitative estimation of the hydrogen environments via deconvolution and the modeling of the spectra.

3.2. Effect of temperature on the hydrogen dynamics in quasicrystals

To investigate the effect of temperature on hydrogen mobility, a variable-temperature NMR experiment was performed for quasicrystals with various H/M at a constant spinning speed of 10 kHz. Fig. 2 shows the spectra for $H/M = 0.7$ and 1.8 (the spectra for other H/M values are shown in Fig. S7 in SI-9). With increasing temperature from 298 to 322 K, the peak width decreases; the

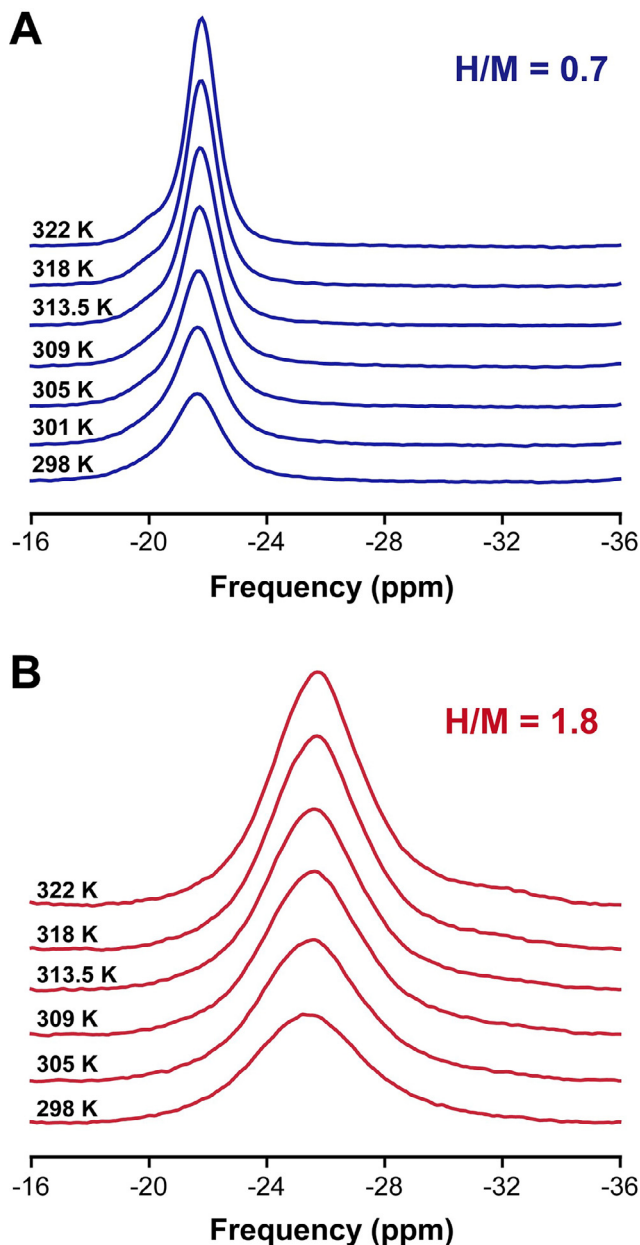


Fig. 2. ^1H MAS NMR spectra of $\text{Ti}_{53}\text{Zr}_{27}\text{Ni}_{20}$ ($\text{H}/\text{M} = 0.7$ and 1.8) quasicrystals upon heating with varying sample temperature as labeled. The FWHM is based on peak maximums. The spinning speed is 10 kHz .

FWHM of the main peak at 322 K for $\text{H}/\text{M} = 0.7$ decreases by $\sim 40\%$ compared to that at 298 K , dropping from 1.9 to 1.2 ppm . The peak widths for $\text{H}/\text{M} = 0.75$ and 0.9 decrease by $\sim 35\%$ and $\sim 30\%$, respectively, as the temperature increases from 298 K to 322 K (see Fig. S7). The observed narrowing of the peak is partly due to the enhanced hydrogen mobility at higher temperatures. The results also confirm that the hydrogen atoms are weakly bound to the interstitial sites of the quasicrystals.

The activation energies (E_a) for hydrogen diffusion at various H/M were obtained from the Arrhenius plot of the temperature dependence of the FWHM of the main peak in the ^1H MAS NMR spectra (Fig. 3). Note that the values represented by the Arrhenius plot in Fig. 3A were calculated based on the FWHM of the main peak only (see SI-3). The estimated activation energies for hydrogen diffusion range from 0.08 to 0.15 eV . For the quasicrystal with $\text{H}/\text{M} = 0.5$, E_a is $\sim 0.1\text{ eV}$. With an increase in the hydrogen

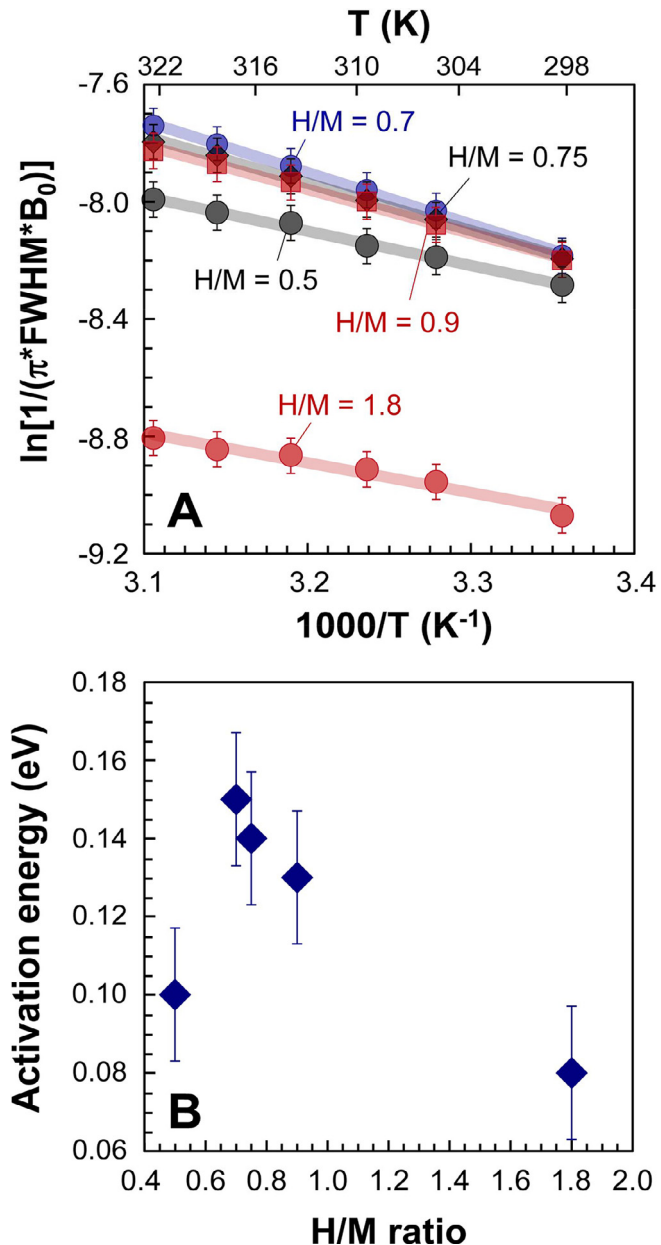


Fig. 3. (A) Effect of temperature on the ^1H main peak width in TiZrNi quasicrystals with varying H/M ratios as labeled. (B) Estimated activation energy barrier (E_a) for hydrogen diffusion in TiZrNi quasicrystals with various H/M ratios.

content, a larger E_a of 0.15 eV is estimated for the sample with a H/M of 0.7 . With increasing hydrogen content, E_a tends to decrease from 0.14 eV (for $\text{H}/\text{M} = 0.75$) to 0.08 eV (for $\text{H}/\text{M} = 1.8$). We note that because of the multiple peaks near the main peak, the estimation of the FWHM and the obtained activation energy for the main peak in the quasicrystal with $\text{H}/\text{M} = 0.5$ may be subject to a moderate degree of uncertainty. This estimated E_a is similar to the estimated values for hydrogen hopping and/or local jumping from NMR spin-lattice (T_1) and spin-echo (T_2) relaxation time measurements (see SI-10) [41]. A further increase in the hydrogen content in the quasicrystals from $\text{H}/\text{M} = 0.7$ to 1.8 may facilitate the diffusion of hydrogen. While further confirmation is necessary, this can be attributed to a weaker binding between hydrogen and metals constituting interstitial tetrahedral sites with increasing number of Ni atoms, as also implied from the reduced magnitude of metal-hydrogen interactions from ^1H NMR spectra.

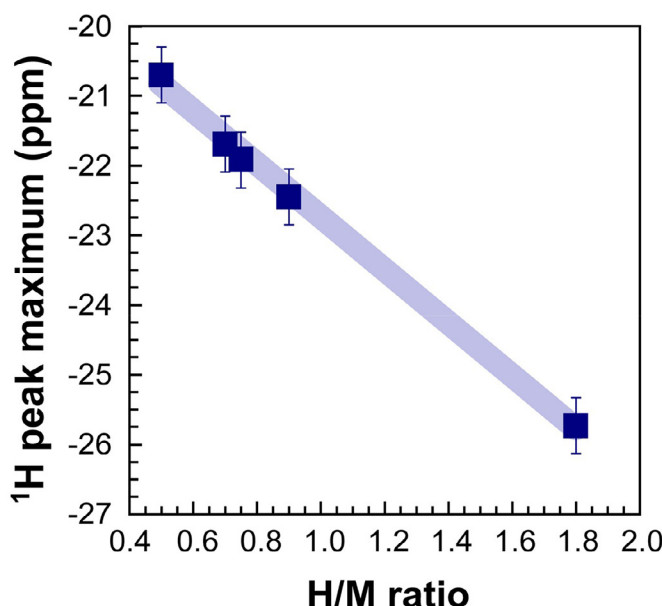


Fig. 4. Variation in the peak maximum in the ¹H MAS NMR spectra for TiZrNi quasicrystals (at 30–35 kHz) with varying H/M ratios. The linear fit of the changes in the ¹H peak maximum with H/M is also shown.

Fast rotor spinning has resulted in an increase in the sample temperature due to frictional heating. The temperature of the sample with varying rotor spinning speeds (from 10 to 35 kHz) was estimated using the ²⁰⁷Pb MAS NMR shift of a Pb(NO₃)₂ sample [56] (see SI-3 and Fig. S2). The results indicate that the change in the main peak width with varying spinning speed is partly due to an increase in the sample temperature. The trends from variable-temperature NMR and frictional heating due to fast sample spinning confirm that the interaction between the hydrogen and adjacent metals is relatively weak, promoting diffusion of hydrogen near ambient temperature conditions.

For the H/M = 1.8 sample, some of the inhomogeneously bound hydrogen atoms have become mobile during heating due to the increase in sample temperature caused by fast sample spinning [69–71]. The spinning speed of 30 kHz, obtained using the 1.9 mm rotor, increases the sample temperature from 296 to ~311 K. The change in the spectrum for H/M = 1.8 is accompanied by the formation of a small amount of hydrogen molecules (see SI-11), as shown in the ¹H MAS NMR spectrum (Fig. S8) that reveals a peak at approximately 4.5 ppm, corresponding to hydrogen molecules [72]. This dehydrogenation is due to the combined effect of fast sample rotation and an increase in the sample temperature, whereas the detailed mechanisms behind this change are not yet clear. Finally, see SI-12 to SI-13 for the ¹H MAS and Hahn echo MAS NMR spectra for rotor and stator backgrounds (Fig. S10), and quasicrystal (Fig. S11) and relevant discussions.

3.3. Quantitative estimation of the hydrogen content in quasicrystals: insights from the ¹H NMR peak shift

Accurate determination of the hydrogen content in hydrogen storage materials is crucial for hydrogen storage applications. The observed peak shift for hydrogen in the ¹H MAS NMR spectrum enables quantification of the hydrogen content in quasicrystals. In particular, Fig. 4 shows the changes in peak shifts with the increase in the H/M ratio, stemming from the varying degree of interactions between hydrogen and the d-electrons in the metal cations. Here, the ¹H peak maximum (σ_K) decreases linearly with increasing hy-

drogen content in the quasicrystal:

$$\sigma_K(\text{ppm}) = -19 - 3.8H/M \quad (1)$$

The simple linear relationship between σ_K and H/M sheds light on a new opportunity to measure the hydrogen content in quasicrystals. While the direct estimation of the hydrogen content in hydrogen-bearing compounds is not trivial, the current results indicate that high-resolution ¹H NMR under fast sample spinning is useful for estimating the hydrogen content in both diverse quasicrystals and metal hydrides.

We note that the peak intensity in the Hahn-echo MAS NMR intensity is not fully quantitative, mainly affected by the spin-spin relaxation times (T_2) of the hydrogen sites (SI-14). The estimated T_2 decreases systematically with increasing H/M (Fig. S12) because of closer proximity between H and Ni with increasing hydrogen content. Therefore, the peak intensity in the Hahn echo NMR spectrum needs to be calibrated taking the changes in T_2 with varying H/M ratio into consideration. However, in the current study the quantitative information comes mainly from the peak position, not from the peak intensity, which shows the clear linear correlation with H/M (Fig. 4).

Our preliminary synchrotron XRD study of Ti₅₃Zr₂₇Ni₂₀ quasicrystals at high pressures of up to 48 GPa revealed that the hydrogen solubility increased with increasing pressure [73]. As solid-state NMR has been used to reveal the pressure-induced structural transitions in diverse diamagnetic materials under compression beyond several GPa [35,74–80], the high-resolution ¹H MAS NMR technique under fast-spinning could also be employed to determine the hydrogen concentrations in pressurized quasicrystals. In addition to traditional probes of the structures and hydrogen contents in quasicrystals, such as XRD [18], volumetric and gravimetric methods [27], and thermal desorption spectroscopy [81], high-resolution ¹H MAS NMR can also be useful for reliable measurement of the hydrogen content in hydrogen storage materials consisting of diverse metal elements and only requires a sample mass of a few mg.

We note that the observed peak shift [Eq. (1)] results from the complex interactions between electrons in metal cations and the hydrogen as indicated by high-resolution ¹H MAS NMR spectra under fast spinning speed (Fig. 1). While the observed trend is expected to be valid for other quasicrystals, the detailed trend may vary with types of metal elements. Further efforts need to be made to explore the nature of hydrogen atoms in other non-crystalline metal alloys with varying compositions. The successful application of the ¹H NMR techniques to the quasicrystals in the current study stems partly from a rather weak paramagnetic interaction within Ti₅₃Zr₂₇Ni₂₀ system. Therefore, its application to other quasicrystals with larger interactions between unpaired electrons and nuclear spins remains. Finally, other NMR methods quantifying direct proximity among protons and nearby metal cations (e.g., [48,80]) can be potentially used to provide additional details of the hydrogen in the quasicrystals.

4. Conclusions

While details on the local structure of host metals surrounding hydrogen atoms are central to understanding the properties relevant to hydrogen storage and release, the lack of such structural information in hydrogen bearing metal alloys and quasicrystals remained the principal impeding factor in the extensive application of these compounds. In this study, we show the potential of ¹H solid-state NMR spectroscopy under fast sample spinning for revealing details of the bonding environment in hydrogenated metal quasicrystals; the first high-resolution ¹H MAS NMR spectra of hydrogenated TiZrNi quasicrystals with varying H/M of 0.5 to 1.8 unveiled the evolution of distinct hydrogen environments in

the quasiperiodic materials. The ^1H main peak position shifts linearly toward a more negative frequency with an increase in the hydrogen content (H/M ratio). Thus, the peak position in the ^1H MAS NMR spectra can be a useful spectral proxy for the hydrogen content in quasicrystals, enabling estimation of the quantities of hydrogen in diverse quasicrystal samples with limited sample volumes.

The current high-resolution ^1H NMR spectroscopy reveals the first direct structures around hydrogen in *non-crystalline metal alloys*. We note that archetypal metal quasicrystal is the major component of technologically important energy materials. Therefore, the unprecedented evidence of the hydrogen configurations of our studies provides atomistic insights into metal alloys and its impact on energy materials. This study sheds light on a new opportunity to prove and resolve hydrogen atom environments in an enormous number of crystalline and non-crystalline energy materials based on metal alloys, such as metal hydrides and quasicrystals for fuel cells and hydrogen storage applications [82,83]. Finally, the current NMR technique will also be potentially helpful in estimating the quantity of hydrogen and natural hydrogen in diverse earth materials with paramagnetic elements [84–86], providing improved prospects for the hydrogen economy.

Declaration of Competing Interest

The authors declare that they have no known competing financial interests or personal relationships that could have appeared to influence the work reported in this paper.

Acknowledgements

This work was supported by the National Research Foundation of Korea (NRF) grant funded by the Ministry of Science and ICT to S. K. Lee (2020R1A3B2079815) and to J. Y. Kim (2021R1A2C1006198). We thank Dr. Jeongjae Lee for helpful discussion. We appreciate two reviewers' constructive comments, which improved the quality and clarity of the manuscript.

Supplementary materials

Supplementary material associated with this article can be found, in the online version, at doi:[10.1016/j.actamat.2022.117657](https://doi.org/10.1016/j.actamat.2022.117657).

References

- [1] D. Shechtman, I. Blech, D. Gratias, J.W. Cahn, Metallic phase with long-range orientational order and no translational symmetry, *Phys. Rev. Lett.* 53 (20) (1984) 1951–1953.
- [2] L. Bindi, P.J. Steinhardt, N. Yao, P.J. Lu, Natural quasicrystals, *Science* 324 (5932) (2009) 1306–1309.
- [3] L. Bindi, J.M. Eiler, Y. Guan, L.S. Hollister, G. MacPherson, P.J. Steinhardt, N. Yao, Evidence for the extraterrestrial origin of a natural quasicrystal, *Proc. Natl. Acad. Sci. U. S. A.* 109 (5) (2012) 1396–1401.
- [4] F. Schurack, J. Eckert, L. Schultz, Synthesis and mechanical properties of cast quasicrystal-reinforced Al-alloys, *Acta Mater.* 49 (8) (2001) 1351–1361.
- [5] G.W. Lee, A.K. Gangopadhyay, K.F. Kelton, Phase diagram studies of Ti-Zr-Ni alloys containing less than 40 at.% Ni and estimated critical cooling rate for icosahedral quasicrystal formation from the liquid, *Acta Mater.* 59 (12) (2011) 4964–4973.
- [6] P.D. Asimow, C. Lin, L. Bindi, C. Ma, O. Tschauner, L.S. Hollister, P.J. Steinhardt, Shock synthesis of quasicrystals with implications for their origin in asteroid collisions, *Proc. Natl. Acad. Sci. U. S. A.* 113 (26) (2016) 7077–7081.
- [7] J.M. Dubois, New prospects from potential applications of quasicrystalline materials, *Mater. Sci. Eng. A* 294–296 (2000) 4–9.
- [8] M. Hirscher, V.A. Yartys, M. Baricco, J. Bellotta von Colbe, D. Blanchard, R.C. Bowman, D.P. Broom, C.E. Buckley, F. Chang, P. Chen, Y.W. Cho, J.C. Crivello, F. Cuevas, W.I.F. David, P.E. de Jongh, R.V. Denys, M. Dornheim, M. Felderhoff, Y. Filinchuk, G.E. Froudakis, D.M. Grant, E.M. Gray, B.C. Hauback, T. He, T.D. Humphries, T.R. Jensen, S. Kim, Y. Kojima, M. Latroche, H.W. Li, M.V. Lototsky, J.W. Makepeace, K.T. Möller, L. Naheed, P. Ngene, D. Noréus, M.M. Nygård, S.I. Orimo, M. Paskevicius, L. Pasquini, D.B. Ravnsbæk, M. Veronica Sofianos, T.J. Udoovic, T. Vegge, G.S. Walker, C.J. Webb, C. Weidenthaler, C. Zlatea, Materials for hydrogen-based energy storage – past, recent progress and future outlook, *J. Alloy. Compd.* 827 (2020) 153548.
- [9] L. Schlapbach, A. Züttel, Hydrogen-storage materials for mobile applications, *Nature* 414 (6861) (2001) 353–358.
- [10] B. Sakintuna, F. Lamaridarkrim, M. Hirscher, Metal hydride materials for solid hydrogen storage: a review, *Int. J. Hydrog. Energy* 32 (9) (2007) 1121–1140.
- [11] H. Shao, G. Xin, J. Zheng, X. Li, E. Akiba, Nanotechnology in Mg-based materials for hydrogen storage, *Nano Energy* 1 (4) (2012) 590–601.
- [12] J. Zhang, Y. Zhu, H. Lin, Y. Liu, Y. Zhang, S. Li, Z. Ma, L. Li, Metal hydride nanoparticles with ultrahigh structural stability and hydrogen storage activity derived from microencapsulated nanoconfinement, *Adv. Mater.* 29 (24) (2017) 1700760.
- [13] A. Schneemann, J.L. White, S. Kang, S. Jeong, L.F. Wan, E.S. Cho, T.W. Heo, D. Prendergast, J.J. Urban, B.C. Wood, M.D. Allendorf, V. Stavila, Nanostructured metal hydrides for hydrogen storage, *Chem. Rev.* 118 (22) (2018) 10775–10839.
- [14] K. Edalati, R. Uehiro, Y. Ikeda, H.W. Li, H. Emami, Y. Filinchuk, M. Arita, X. Sauvage, I. Tanaka, E. Akiba, Z. Horita, Design and synthesis of a magnesium alloy for room temperature hydrogen storage, *Acta Mater.* 149 (2018) 88–96.
- [15] M.M. Nygård, Ø.S. Fjellvåg, M.H. Sørby, K. Sakaki, K. Ikeda, J. Armstrong, P. Va-jeeston, W.A. Slawiński, H. Kim, A. Machida, Y. Nakamura, B.C. Hauback, The average and local structure of $\text{TiV}_{x}\text{CrNbD}_x$ ($x=0, 2.2, 8$) from total scattering and neutron spectroscopy, *Acta Mater.* 205 (2021) 116496.
- [16] Y. Liu, Z. Zhu, F. Liu, J. Xu, Nonlinear dynamic characteristics and bifurcation analysis of $\text{Ti}-\text{Zr}-\text{Ni}$ quasicrystal as hydrogen storage material, *Int. J. Hydrog. Energy* 46 (31) (2021) 16667–16675.
- [17] J.Y. Kim, P.C. Gibbons, K.F. Kelton, Hydrogenation of Pd-coated samples of the Ti-Zr-based icosahedral phase and related crystalline phases, *J. Alloy. Compd.* 266 (1–2) (1998) 311–317.
- [18] S.H. Lee, J. Kim, Structure and hydrogen absorption properties of $\text{Ti}_{53}\text{Zr}_{27}\text{Ni}_{20}$ (Pd,V) quasicrystals, *Int. J. Hydrog. Energy* 43 (41) (2018) 19130–19140.
- [19] J.Y. Kim, R. Hennig, V.T. Huett, P.C. Gibbons, K.F. Kelton, Hydrogen absorption in Ti-Zr-Ni quasicrystals and 1/1 approximants, *J. Alloy. Compd.* 404–406 (2005) 388–391.
- [20] K.F. Kelton, J.J. Hartzell, R.G. Hennig, V.T. Huett, A. Takasaki, Hydrogen storage in Ti-Zr and Ti-Hf-based quasicrystals, *Philos. Mag.* 86 (6–8) (2006) 957–964.
- [21] A.M. Viano, R.M. Stroud, P.C. Gibbons, A.F. McDowell, M.S. Conrad, K.F. Kelton, Hydrogenation of titanium-based quasicrystals, *Phys. Rev. B Condens. Matter* 51 (17) (1995) 12026–12029.
- [22] A. Shastri, E.H. Majzoub, F. Borsa, P.C. Gibbons, K.F. Kelton, ^1H NMR study of hydrogen in quasicrystalline $\text{Ti}_{0.45-x}\text{V}_x\text{Zr}_{0.38}\text{Ni}_{0.17}$, *Phys. Rev. B* 57 (9) (1998) 5148–5153.
- [23] A. Sadoc, J.Y. Kim, K.F. Kelton, Local atomic order in icosahedral Ti-Zr-Ni and hydrogenated Ti-Zr-Ni quasicrystals, *Philos. Mag. A* 79 (11) (1999) 2763–2772.
- [24] A. Takasaki, K. Kelton, Hydrogen storage in Ti-based quasicrystal powders produced by mechanical alloying, *Int. J. Hydrog. Energy* 31 (2) (2006) 183–190.
- [25] R.G. Hennig, E.H. Majzoub, K.F. Kelton, Location and energy of interstitial hydrogen in the 1/1 approximant W-TiZrNi of the icosahedral TiZrNi quasicrystal: rietveld refinement of x-Ray and neutron diffraction data and density-functional calculations, *Phys. Rev. B* 73 (18) (2006) 184205.
- [26] H. Huang, D.Q. Meng, X.C. Lai, T.W. Liu, Y. Long, Q.M. Hu, Structure of Bergman-type W-TiZrNi approximants to quasicrystal, analyzed by lattice inversion method, *J. Phys. Condens. Matter* 26 (31) (2014) 315003.
- [27] T.Y. Wei, K.L. Lim, Y.S. Tseng, S.L.I. Chan, A review on the characterization of hydrogen in hydrogen storage materials, *Renew. Sustain. Energy Rev.* 79 (2017) 1122–1133.
- [28] X. Xue, M. Kanzaki, Structure of hydrous aluminosilicate glasses along the diopside-anorthite join: a comprehensive one- and two-dimensional ^1H and ^{27}Al NMR study, *Geochim. Cosmochim. Acta* 72 (9) (2008) 2331–2348.
- [29] S.Y. Kim, W.H. Suh, J.H. Choi, Y.S. Yi, S.K. Lee, G.D. Stucky, J.K. Kang, Template-free synthesis of high surface area nitrogen-rich carbon microporous spheres and their hydrogen uptake capacity, *J. Mater. Chem. A* 2 (7) (2014) 2227–2232.
- [30] J.F. Stebbins, Toward the wider application of ^{29}Si NMR spectroscopy to paramagnetic transition metal silicate minerals: copper(II) silicates, *Am. Mineral.* 102 (12) (2017) 2406–2414.
- [31] J.F. Stebbins, X. Xue, NMR spectroscopy of inorganic earth materials, *Rev. Mineral. Geochem.* 78 (1) (2014) 605–653.
- [32] H.I. Kim, S.K. Lee, The degree of polymerization and structural disorder in $(\text{Mg},\text{Fe})\text{SiO}_3$ glasses and melts: insights from high-resolution ^{29}Si and ^{17}O solid-state NMR, *Geochim. Cosmochim. Acta* 250 (2019) 268–291.
- [33] M.J. Duer, Solid State NMR Spectroscopy: Principles and Applications, Wiley, 2008.
- [34] H. Eckert, Structural characterization of noncrystalline solids and glasses using solid-state NMR, *Prog. Nucl. Magn. Reson. Spectrosc.* 24 (3) (1992) 159–293.
- [35] S.K. Lee, K.Y. Mun, Y.H. Kim, J. Lhee, T. Okuchi, J.F. Lin, Degree of permanent densification in oxide glasses upon extreme compression up to 24 GPa at room temperature, *J. Phys. Chem. Lett.* 11 (8) (2020) 2917–2924.
- [36] T. Misaki, I. Oikawa, H. Takamura, Negative knight shift in Ba-Ti oxyhydride: an indication of the multiple hydrogen occupation, *Chem. Mater.* 31 (18) (2019) 7178–7185.
- [37] C. Korn, NMR study comparing the electronic structures of ZrH_x and TiH_x , *Phys. Rev. B* 28 (1) (1983) 95–111.
- [38] C.P. Slichter, Principles of Magnetic Resonance, Springer, Berlin, 1990.
- [39] K.R. Faust, D.W. Pitsch, N.A. Stojanovich, A.F. McDowell, N.L. Adolphi, E.H. Majzoub, J.Y. Kim, P.C. Gibbons, K.F. Kelton, NMR second-moment study of hydrogen sites in icosahedral $\text{Ti}_{45}\text{Zr}_{38}\text{Ni}_{17}$ quasicrystals, *Phys. Rev. B* 62 (17) (2000) 11444–11449.

- [40] G. Lasanda, P. Bánki, K. Tompa, ^1H NMR spectra and H-site occupancy in $\text{Zr}_{0.5}\text{Cu}_{0.5-y}\text{H}_1$ metallic glasses, Solid State Commun. 87 (8) (1993) 665–668.
- [41] A. Kocjan, S. Kováč, A. Gradišek, J. Kováč, P.J. McGuiness, T. Apih, J. Dolinšek, S. Kobe, Selective hydrogenation of Ti-Zr-Ni alloys, Int. J. Hydrot. Energy 36 (4) (2011) 3056–3061.
- [42] A. Gradišek, T. Apih, Hydrogen dynamics in partially quasicrystalline $\text{Zf}_{0.9}\text{Cu}_{12}\text{Ni}_{11}\text{Al}_{75}$: a fast field-cycling relaxometric study, J. Phys. Chem. C 119 (19) (2015) 10677–10681.
- [43] M.G. Shelyapina, A.V. Vyvodtceva, K.A. Klyukin, O.O. Bavrina, Y.S. Chernyshev, A.F. Privalov, D. Fruchart, Hydrogen diffusion in metal-hydrogen systems via NMR and DFT, Int. J. Hydrot. Energy 40 (47) (2015) 17038–17050.
- [44] M. Deschamps, F. Fayon, S. Cadars, A.L. Rollet, D. Massiot, ^1H and ^{19}F ultra-fast MAS double-quantum single-quantum NMR correlation experiments using three-spin terms of the dipolar homonuclear Hamiltonian, Phys. Chem. Chem. Phys. 13 (17) (2011) 8024–8030.
- [45] S.P. Brown, Applications of high-resolution ^1H solid-state NMR, Solid State Nucl. Magn. Reson. 41 (2012) 1–27.
- [46] S.R. Chaudhari, J.M. Griffin, K. Broch, A. Lesage, V. Lemaury, D. Dudenko, Y. Olivier, H. Sirringhaus, L. Emsley, C.P. Grey, Donor-acceptor stacking arrangements in bulk and thin-film high-mobility conjugated polymers characterized using molecular modelling and MAS and surface-enhanced solid-state NMR spectroscopy, Chem. Sci. 8 (4) (2017) 3126–3136.
- [47] H. Kim, J.S. Kim, J.M. Heo, M. Pei, I.H. Park, Z. Liu, H.J. Yun, M.H. Park, S.H. Jeong, Y.H. Kim, J.W. Park, E. Oveisí, S. Nagane, A. Sadhanala, L. Zhang, J.J. Kweon, S.K. Lee, H. Yang, H.M. Jang, R.H. Friend, K.P. Loh, M.K. Nazeeruddin, N.G. Park, T.W. Lee, Proton-transfer-induced 3D/2D hybrid perovskites suppress ion migration and reduce luminance overshoot, Nat. Commun. 11 (1) (2020) 3378.
- [48] J. Lee, W. Lee, K. Kang, T. Lee, S.K. Lee, Layer-by-layer structural identification of 2D Ruddlesden-Popper hybrid lead iodide perovskites by solid-state NMR spectroscopy, Chem. Mater. 33 (1) (2020) 370–377.
- [49] Y. Nishiyama, Fast magic-angle sample spinning solid-state NMR at 60–100 kHz for natural abundance samples, Solid State Nucl. Magn. Reson. 78 (2016) 24–36.
- [50] P.J. Sideris, U.G. Nielsen, Z.H. Gan, C.P. Grey, Mg/Al ordering in layered double hydroxides revealed by multinuclear NMR spectroscopy, Science 321 (5885) (2008) 113–117.
- [51] S. Wi, R. Schurko, L. Frydman, ^1H - ^2H cross-polarization NMR in fast spinning solids by adiabatic sweeps, J. Chem. Phys. 146 (10) (2017) 104201.
- [52] R. Zhang, K.H. Mroue, A. Ramamoorthy, Proton-based ultrafast magic angle spinning solid-state NMR spectroscopy, Acc. Chem. Res. 50 (4) (2017) 1105–1113.
- [53] J.Y. Kim, Magnetic properties of Ti-Zr-Ni quasicrystals, J. Korean Phys. Soc. 53 (3) (2008) 1593–1596.
- [54] J.J. Kweon, R. Fu, E. Steven, C.E. Lee, N.S. Dalal, High field MAS NMR and conductivity study of the superionic conductor LiH_2PO_4 : critical role of physisorbed water in its protonic conductivity, J. Phys. Chem. C 118 (25) (2014) 13387–13393.
- [55] J.J. Kweon, R. Fu, J.A. Kitchen, P.L. Gor'kov, W.W. Brey, N.S. Dalal, Evidence from 900 MHz ^1H MAS NMR of displacive behavior of the model order-disorder antiferroelectric $\text{NH}_4\text{H}_2\text{AsO}_4$, J. Phys. Chem. C 119 (9) (2015) 5013–5019.
- [56] A. Bielecki, D.P. Burum, Temperature dependence of ^{207}Pb MAS spectra of solid lead nitrate. An accurate, sensitive thermometer for variable-temperature MAS, J. Magn. Reson. A 116 (1995) 215–220.
- [57] R.C. Bowman, E.L. Venturini, B.D. Craft, A. Attalla, D.B. Sullenger, Electronic structure of zirconium hydride: a proton NMR study, Phys. Rev. B 27 (3) (1983) 1474–1488.
- [58] R. Göring, R. Lukas, K. Bohmhammel, Multipulse NMR investigation of band structure in titanium hydride: proton knight shift and spin-lattice relaxation, J. Phys. C Solid State Phys. 14 (36) (1981) 5675–5687.
- [59] W.J. Kim, P.C. Gibbons, K.F. Kelton, W.B. Yelon, Structural refinement of 1/1 bcc approximants to quasicrystals: Bergman-type $W(\text{TiZrNi})$ and Mackay-type $M(\text{TiZrFe})$, Phys. Rev. B 58 (5) (1998) 2578–2585.
- [60] R.G. Hennig, K.F. Kelton, A.E. Carlsson, C.L. Henley, Structure of the icosahedral Ti-Zr-Ni quasicrystal, Phys. Rev. B 67 (13) (2003) 134202.
- [61] H.I. Kim, S.K. Lee, Extent of disorder in iron-bearing albite and anorthite melts: insights from multi-nuclear (^{29}Si , ^{27}Al , and ^{17}O) solid-state NMR study of iron-bearing $\text{NaAlSi}_3\text{O}_8$ and $\text{CaAl}_2\text{Si}_2\text{O}_8$ glasses, Chem. Geol. 538 (2020) 119498.
- [62] A. Sadoc, E.H. Majzoub, V.T. Huett, K.F. Kelton, Local structure in hydrogenated Ti-Zr-Ni quasicrystals and approximants, J. Alloy. Compd. 356–357 (2003) 96–99.
- [63] S.S. Sidhu, L. Heaton, D.D. Zauberis, Neutron diffraction studies of hafnium-hydrogen and titanium-hydrogen systems, Acta Cryst. 9 (6) (1956) 607–614.
- [64] S.H. Lee, A. Huq, W. Yang, J. Kim, Analysis of local sites of deuterium in $\text{Ti}_{53}\text{Zr}_{27}\text{Ni}_{20}$ alloys, Phys. B Condens. 551 (2018) 33–36.
- [65] M. Carravetta, Y. Murata, M. Murata, I. Heinmaa, R. Stern, A. Tontcheva, A. Samoson, Y. Rubin, K. Komatsu, M.H. Levitt, Solid-state NMR spectroscopy of molecular hydrogen trapped inside an open-cage fullerene, J. Am. Chem. Soc. 126 (13) (2004) 4092–4093.
- [66] S. Mamone, M. Concistre, I. Heinmaa, M. Carravetta, I. Kuprov, G. Wall, M. Denning, X. Lei, J.Y. Chen, Y. Li, Y. Murata, N.J. Turro, M.H. Levitt, Nuclear magnetic resonance of hydrogen molecules trapped inside C_70 fullerene cages, ChemPhysChem 14 (13) (2013) 3121–3130.
- [67] M.S. Conradi, M.P. Mendenhall, T.M. Ivancic, E.A. Carl, C.D. Browning, P.H.L. Notten, W.P. Kalisvaart, P.C.M.M. Magusin, R.C. Bowman, S.J. Hwang, N.L. Adolph, NMR to determine rates of motion and structures in metal-hydrides, J. Alloy. Compd. 446–447 (2007) 499–503.
- [68] H.N. Kim, S.K. Lee, Atomic structure and dehydration mechanism of amorphous silica: insights from ^{29}Si and ^1H solid-state MAS NMR study of SiO_2 nanoparticles, Geochim. Cosmochim. Acta 120 (2013) 39–64.
- [69] R.N. Purusottam, G. Bodenhausen, P. Tekely, Determination of sample temperature in unstable static fields by combining solid-state ^{79}Br and ^{13}C NMR, J. Magn. Reson. 246 (2014) 69–71.
- [70] K. Elbayed, B. Dillmann, J. Raya, M. Piotto, F. Engelke, Field modulation effects induced by sample spinning: application to high-resolution magic angle spinning NMR, J. Magn. Reson. 174 (1) (2005) 2–26.
- [71] T. Hao, M. Ono, S. Okayasu, S. Sakai, K. Narumi, Y. Hiraiwa, H. Naramoto, Y. Maeda, RBS study of diffusion under strong centrifugal force in bimetallic Au/Cu thin films, Nucl. Instrum. Methods Phys. Res. B 268 (11–12) (2010) 1867–1870.
- [72] H. Fujiwara, J. Yamabe, S. Nishimura, Determination of chemical shift of gas-phase hydrogen molecules by ^1H nuclear magnetic resonance, Chem. Phys. Lett. 498 (1–3) (2010) 42–44.
- [73] J. Kim, S.H. Lee, W. Yang, Hydrogen storage and transport properties of TiZrNi quasicrystals under high pressure, in: Proceedings of the 14th International Conference on Quasicrystals, Krnska Gora, Slovenia, 2019, p. 62.
- [74] E.J. Kim, Y.H. Kim, S.K. Lee, Pressure-induced structural transitions in Na-Li silicate glasses under compression, J. Phys. Chem. C 123 (43) (2019) 26608–26622.
- [75] X. Xue, J.F. Stebbins, M. Kanzaki, Correlations between ^{17}O NMR parameters and local structure around oxygen in high-pressure silicates: implications for the structure of silicate melts at high pressure, Am. Mineral. 79 (1994) 31–42.
- [76] J.R. Allwardt, J.F. Stebbins, B.C. Schmidt, D.J. Frost, A.C. Withers, M.M. Hirschmann, Aluminum coordination and the densification of high-pressure aluminosilicate glasses, Am. Mineral. 90 (7) (2005) 1218–1222.
- [77] S.K. Lee, K. Mibe, Y. Fei, G.D. Cody, B.O. Mysein, Structure of B_2O_3 glass at high pressure: a ^{11}B solid-state NMR study, Phys. Rev. Lett. 94 (16) (2005) 165507.
- [78] S.J. Gaudio, C.E. Lesher, H. Maekawa, S. Sen, Linking high-pressure structure and density of albite liquid near the glass transition, Geochim. Cosmochim. Acta 157 (2015) 28–38.
- [79] S.K. Lee, J.L. Mosenfelder, S.Y. Park, A.C. Lee, P.D. Asimow, Configurational entropy of basaltic melts in earth's mantle, Proc. Natl. Acad. Sci. U. S. A. 117 (36) (2020) 21938–21944.
- [80] S.K. Lee, A.C. Lee, J.J. Kweon, Probing medium-range order in oxide glasses at high pressure, J. Phys. Chem. Lett. 12 (4) (2021) 1330–1338.
- [81] F. von Zeppelin, M. Haluška, M. Hirscher, Thermal desorption spectroscopy as a quantitative tool to determine the hydrogen content in solids, Thermochim. Acta 404 (1–2) (2003) 251–258.
- [82] M.V. Lototsky, I. Tolj, L. Pickering, C. Sita, F. Barbir, V. Yartys, The use of metal hydrides in fuel cell applications, Prog. Nat. Sci. 27 (1) (2017) 3–20.
- [83] S. de Graaf, J. Momand, C. Mitterbauer, S. Lazar, B.J. Kooi, Resolving hydrogen atoms at metal-metal hydride interfaces, Sci. Adv. 6 (2020) eaay4312.
- [84] E. Drobner, H. Huber, G. Wächtershäuser, D. Rose, K.O. Stetter, Pyrite formation linked with hydrogen evolution under anaerobic conditions, Nature 346 (1990) 742–744.
- [85] A. Kolesnikov, V.G. Kutcherov, A.F. Goncharov, Methane-derived hydrocarbons produced under upper-mantle conditions, Nat. Geosci. 2 (8) (2009) 566–570.
- [86] V. Zgonnik, The occurrence and geoscience of natural hydrogen: a comprehensive review, Earth Sci. Rev. 203 (2020) 103140.